Towards Statistical Inferences of Successful Prostate Surgery

Frederic McKenzie[1], Jose Diaz[2], Paul Schellhammer[2], Rania Hussein[1]
[1]Electrical and Computer Engineering Department, Old Dominion University, VA, USA
[2] Urology and Pathology Departments, Eastern Virginia Medical School, VA, USA

Abstract— **Prostate cancer continues to be the leading cancer in the United States male population. The options for local therapy have proliferated and include various forms of radiation delivery, cryo-destruction, and novel forms of energy delivery as in high-intensity focused ultrasound. Surgical removal, however, remains the standard procedure for cure. Currently there are little objective parameters that are used to compare the efficiency of each form of surgical removal. As surgeons apply these different surgical approaches, a quality assessment would be most useful, not only with regard to overall comparison of one approach vs. another but also surgeon evaluation of personal surgical performance as they relate to a standard. To this end, we discuss the development of a process employing image reconstruction and analysis techniques to assess the volume and extent of extracapsular soft tissue removed with the prostate. Parameters such as the percent of capsule covered by soft tissue and where present the average depth of soft tissue coverage are assessed. A final goal is to develop software for the purpose of a quality assurance assessment for pathologists and surgeons to evaluate the adequacy/appropriateness of each surgical procedure; laparoscopic versus open perineal or retropubic prostatectomy.**

Keywords—**image reconstruction, 3D image quantitation, prostate surgery assessment**

I. Introduction

Prostate cancer is one of the leading causes of cancer death among the male population in the United States. Early detection of the disease is much more common nowadays than in the past. Nevertheless, radical prostatectomy still remains a preferred method of treatment. Currently there are little objective parameters that are used to compare the efficiency of one form of surgical removal over another. An objective methodology that could be applied to surgical specimens would be of immense value to establish clinical trial criteria for skills assessment, for trial entry, for ongoing assessment during trial conduct, and finally for dissemination of a mechanism of quality control and reassessment of individual surgical practices.

A novel methodology to computerize and objectively quantify the assessment process is to utilize a 3D reconstructed model for the prostate gland. With such a model, the curvature of the capsule, the irregular borders of the extra-capsular tissues as well as the extensions of the tumor can be visualized. Additionally, software algorithms may be designed and applied to quantitate the virtual model. In general, the reconstruction process consists of three main steps: a) extracting the prostate image contours, b) aligning given contours and interpolating intermediate contours, and c) reconstructing surfaces or volumes. During the last decade, there has been a considerable amount of research in the visualization and the 3D reconstruction of medical data [3-11]. Most research focused on developing or improving algorithms that consider the last two steps of the reconstruction process.

Three-dimensional reconstruction has led to the formation of 3D physical biomodels, which greatly facilitates characterization, analysis and simulation of tissue structures. The continuing evolution of 3D and visualization imaging promises even greater capabilities for accurate noninvasive clinical diagnoses and treatment, as well as for quantitative biological investigations and scientific exploration, targeted at ever increasing the understanding of the human condition and how to improve it. In the near future, 3D imaging will be commonly integrated in surgical suites with imaging instrumentation, which will allow surgeons to probe tissue intra-operatively and view detailed soft-tissue anatomy in real time while performing interventional procedures.

II. Methodology

Over the past year, we have been developing a process using software algorithms to assess the percentage and depth of extra-capsular soft tissue removed with the prostate. We were provided with images of prostate slices by the Pathology Department at Eastern Virginia Medical School (EVMS). The test images were taken from traditionally processed prostate slices where a pathologist would simply slice the prostate at imprecise intervals and place these slices on microscope slides. Since normal microscope slides are too narrow for a whole mount of the prostate slice; these slices are further divided so that they may fit on the microscope slides. As a result, after image capture, each prostate slice image consists of about four to six parts that are combined to form one slice. The raison d'être is the prostate capsule boundary that differentiates the extra-capsular tissue. This boundary's contour is determined by a time-consuming hand-drawn line placed on a separate layer to the slice information in the image (Figure 1).

The hand-drawn boundary may be seen in yellow in Figure 1. It should be noted that the yellow line is approx 1.1 mm thick and, therefore, one source of error. This line represents a contour used to construct the 3D prostate capsule model. The extraprostatic tissue contours were taken as the continuous perimeter of the outer surface of the scanned prostate slices.

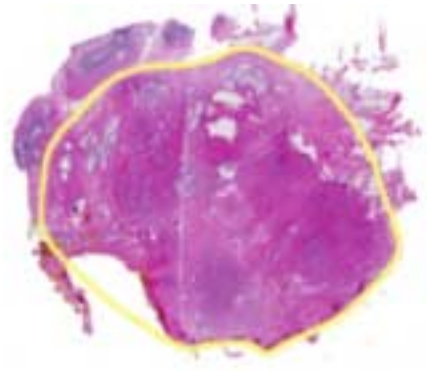

Figure 1: A prostate slice with the hand-drawn capsule boundary

For the initial prostate data, nine contours were generated this way and are separated from the capsular contours.

Thus, each slice's image file is manipulated to create 2 additional files, one conveys the gland boundary information and the other conveys the extraprostatic tissue boundary information. These files are then read into a 3D modeling package to extrapolate a geometric curve. The series of curves derived from all the slices' images are skinned and lofted together to reconstruct a 3D model of the prostate using the urethra and prostate shape as guides. The distance between the consecutive polygonal curves was arbitrarily decided to be of approximately 5.33 mm. In this last stage of the reconstruction phase, a triangular, polygonal mesh surface is created, resulting in a capsule model and an extraprostatic tissue model. Figure 2a represents the skinned capsule with yellow (lighter) portions representing the extraprostatic tissue coverage. The quantitation of this coverage percentage may be gained by polygonal surface calculation or by point cloud estimation. The results discussed here uses point cloud estimation where, after reconstruction, a point cloud bounded by the reconstructed meshes was generated for both the capsule and the extraprostatic models (Figure 2b). Polygonal surface estimation will be an additional method used to further validate results.

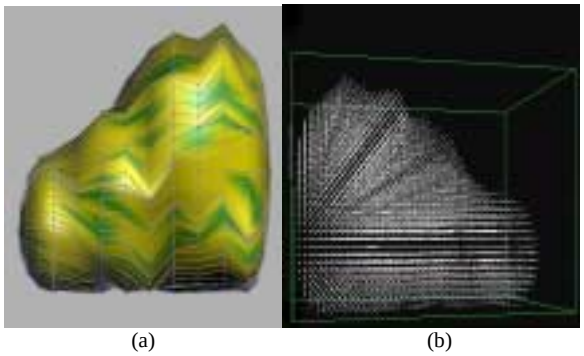

(a) (b)

Figure 2: Reconstructed prostate model and corresponding point cloud

A. Calculating the Percentage of Coverage

Two separate point cloud files were generated to represent both the gland and extraprostatic tissue models. Each of these files was read into a separate matrix and then mapped to one 3D matrix. The location of each point in the gland matrix was mapped to its corresponding point in the 3D matrix by the following equations:

xloc = (a.x/1.2)*xsize + xoffset xoffset = morenegX *xsize
yloc = (a.y/1.2)*ysize + yoffset yoffset = morenegY *ysize
zloc = (a.z/2.4)*zsize + zoffset zoffset = morenegZ *zsize

Where

- Xloc,yloc,zloc are the x,y,z coordinates of the 3D matrix,
- a.x,a.y,a.z are the values of the coordinates of the current point in the gland matrix,
- xsize,ysize,zsize are the maximum sizes of the 3D matrix in the x,y,z-directions
- morenegX, morenegY, morenegZ are the absolute values of the greatest negative value in the x,y,z-directions.
- The values of 1.2,1.2, 2.4 are the length of the model in generic units in the x,y,z-directions respectively.

Once the location of a point was calculated, a value was assigned to that location of the matrix. So the 3D matrix then contained values for the gland and other values for the extraprostatic tissue. The 3D matrix was traversed until a point on the surface of the capsule was encountered. Subsequently, a neighborhood check for extraprostatic tissue points was performed. The extraprostatic tissue points encountered in this manner increased the count of covered gland points while also contributing to the total number of gland points encountered (covered or uncovered). The ratio of these counts provided the percentage of extra-capsular tissue coverage for a particular prostate. We performed both an 8 neighbor (Moore neighborhood) check of the gland point as well a 4 neighbor von Neumann check.

III. RESULTS

From the results in the table below, we note that there is a difference of about 11% between the 4 neighbors and the 8 neighbors check. This is because in some cases the 4 neighbors check fails to detect a covered point while it can be detected by the 8 neighbors. These cases occur when the 8 neighbors check considers an extraprostatic tissue point located to one of the diagonals as a covering point while the 4 neighbors considers only the 4 sides of the point. Actually whether or not to consider the diagonals is not an issue. It is believed that the two methods serve to bound the true percentage coverage. Although, it should be noted that this

model, developed from the traditional slicing method, contains a significant amount of noisy data.

TABLE I
POINT CLOUD RESULTS AT TWO DENSITIES

	Model constructed using 50*50*100 divisions	Denser point cloud using 100*100*200 divisions
# of original capsule points	15882	126187
# of original extraprostatic (EP) points	19699	155948
# of capsule points after mapping	14688	121293
# of EP tissue points after mapping	7210	58684
# of capsule points on the surface	1964	8200
# of capsule points covered (4 neighbor)	1525	6411
# of capsule points covered (8 neighbor)	1753	7309
% Coverage (4 neighbor)	77.6477	78.1829
% Coverage (8 neighbor)	89.2566	89.1341

Currently, a new protocol is being used which should enhance the appearance and definition of the slice contours, reduce noise in the data, and hence improve results. The whole gland is sliced at regular intervals and mounted on microscope slides that are sufficiently large enough to hold the complete slice. This "whole mount" approach is a well known procedure and is currently in practice at EVMS.

IV. FUTURE EFFORTS

The whole-mount prostate specimens prepared by a uropathologist will be eventually scanned to produce digital images. As before, each slice's image file will be manipulated to create 2 additional files, one conveys the capsule information and the other conveys the extraprostatic tissue information. After reconstruction, a point cloud bounded by the reconstructed meshes will be generated for both the capsule and the extraprostatic models. This information will be then exported to data files where software algorithms use differences of the point clouds and of polygonal meshes to quantitate coverage, depth, and volumes.

Software algorithms will be developed to perform automatic recognition of the prostate capsule and outer parenchymal contour. Currently, this is tediously done by pathologists in order to facilitate 3D reconstruction of the prostate capsule and extra-capsular tissue. Because of the problems caused by the manual determination of the gland boundary, this research will also focus on developing an algorithm that automatically determines it. The determination of this boundary can be done by recognition of the histological wavy pattern of the elastic and collagenous fibers within the prostate capsule as well as the identification of the loose connective tissue and fat present in the extraprostatic tissue immediately out of the capsule (Figure 3). This can be clearly recognized under the microscope but also under high resolution of the scanned digital images. However, the prostate capsule is often times unrecognizable because of the naturally occurring intrusion of muscle into the prostate gland at the anterior apex and fusion of extraprostatic connective tissue with the prostate gland at its base. At these regions where the prostate capsule disappears, its contours will be arbitrarily reconstructed by drawing a continuing contour line at those areas where the capsule can be objectively recognized and based on the natural shape of the prostate gland.

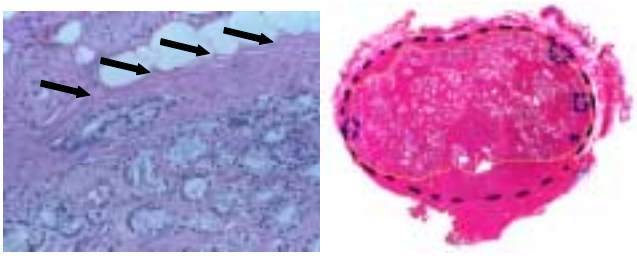

Figure 3: Wavy Pattern (left); Parenchymal Outer Contour (light yellow line on right)

In addition, another surrogate parameter, which is pertinent to the quality of the surgery and clinical outcome will be created. We define this parameter as the parenchymal outer contour. This parameter represents the outer contour of the prostatic glandular epithelial elements, which is the histological compartment where cancer originates. The thin yellow line in Figure 3 illustrates this parameter.

The shape of the prostate profile and the urethral location will also be for centering and assembling the digital images. This will require the images to be scanned at a very high resolution to capture these fine details of the tissue. A variety of image processing techniques will be investigated to determine which of them is applicable. Also, there are mathematical equations that will be used to provide a standard prostate shape at various stages (Figure 4). This mathematical model can help in the shape determination part of the problem. Shape models have frequently been used in determining anatomy. Fitton et al [7] used a Hough transform to automatically assess the regional systolic thickening of the left ventricle from cardiac wall segmentation. They found an initial approximation of the epicardial boundary where they approximated the shape of the epicardial contour with a circle. The Hough transform was used to detect the circle parameters then twenty control points were placed uniformly along the estimated circle boundary for further boundary refinement. This method has its limitations in terms of the time required by the Hough transform. Nevertheless, the idea of approximating the boundary with a circle is similar to the idea of our mathematical model, this model also approximates the shape of the prostate to a standard model.

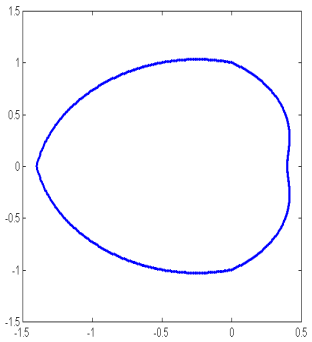

Figure 4. Mathematically Produced Prostate Shape

V. Conclusion

The use of 3D visualization and quantitation techniques is widely used in medical applications. In fact, there are a number of relevant research efforts relevant to the work proposed here. For example, Xu et al [4] describes a robust fuzzy segmentation algorithm that could play a part in an adaptive image processing methodology for the automatic detection of the prostate capsule. Also, Gaita et al [6] applies an edge detection algorithm in finding orthogonal sections to reconstruct 3D objects. While Basset et al [5] reconstructed prostates by using a triangulation method that approximates the surface between two consecutive slices by a collection of planar triangular patches. This method is rapid and satisfies the representations of anatomic shapes like the prostate. Such a method might prove useful in someday applying this research to performance-oriented applications like image-guided surgery.

3D edge detection and pattern recognition techniques have been used for the automatic delineation of neighboring tissues in medical data [8, 9]. However, since determining the prostate capsule depends on many factors like the wavy patterns, urethra location, parenchymal line as well as the shape, it cannot be completely solved by only applying such clean cut techniques. An adaptive imaging technique is needed to automatically delineate prostate capsules using an integration of these varied techniques.

Other work might prove useful in evaluating tumor volumes. Adiga & Chaudhuri [10] described a grading system for the prostate cancer based on 3D histopathological images.

The quantitation methodology described previously will be reused and adapted to the whole-mount protocol in future efforts. This method is also described in [1,2]. Validation of results will concern the use of real volume data compared to measurements obtained from computer models to determine potential differences between real and virtual values.

Acknowledgment

The authors would like to thank the Center for Specialized Surgery and the Virginia Prostate Center.

References

[1] McKenzie, Frederic D., Rania Hussein, Paul Schellhammer, Jose Diaz. “Quantifying Prostate Surgery Success through 3D Reconstruction and Measurement.” The 11th Annual Medicine Meets Virtual Reality (MMVR) Conference. Poster presentation. Newport Beach, California. January 22- 25,2003.

[2] McKenzie, Frederic D., Rania Hussein, Jennifer Seevinck, Paul Schellhammer, Jose Diaz. “Prostate Gland and Extra-Capsular Tissue 3D Reconstruction and Measurement.” The 3rd IEEE symposium on Bioinformatics and Bioengineering (BIBE), Bethesda, Maryland. March 10-12, 2003. Pages 246-250.

[3] Xuan, J. Sesterhenn I., HayesWS,Wang Y., Adali T., Yagi Y, Freedman M.T, Mun S.K. (1998). “Surface Reconstruction and Visualization of the surgical prostate model” Proceedings of the SPIE Medical Imaging Conference, 1997, 3031: 50–61.

[4] C. Xu, D. L. Pham, M. E. Etemad, D. N. Yu, and J. L. Prince, "Reconstruction of the Central Layer of the Human Cerebral Cortex from MR images," in Proc. of the First International Conference on Medical Image Computing and Computer Assisted Interventions (MICCAI'98), pp. 482-488, 1998

[5] Basset O, Dautraix Ricard I, Gimenez G, Mestas JL. Three-dimensional reconstruction of the prostate from transverse or sagittal ultrasonic images. Proceedings of SPIE, vol.1771, 1993, pp.559-66. USA.

[6] Crivianu-Gaita D, Miclea F, Gaspar A, Margineatu D, Holban S. 3D reconstruction of prostate from ultrasound images. International Journal of Medical Informatics, vol.45, no.1-2, June 1997, pp.43-51. Publisher: Elsevier, Ireland.

[7] Fitton I, Shen J, Perron J-M, Kerouani A, Roudaut R, Barat J-L. Regional myocardial wall thickening of the left ventricle from segmentation of echocardiographic images. Proceedings of SPIE - the International Society for Optical Engineering, vol.4549, 2001, pp.58-63. USA.

[8] Kshirsagar A, Watson PJ, Herrod NJ, Tyler JA, Hall LD. Quantitation of articular cartilage dimensions by computer analysis of 3D MR images of human knee joints. Proceedings of the 19th Annual International Conference of the IEEE Engineering in Medicine and Biology Society. (Cat. No.97CH36136). IEEE. Part vol.2, 1997, pp.753-6 vol.2. Piscataway, NJ, USA.

[9] Vaidyanathan M, Velthuizen R, Clarke LP, Hall LO. Quantitation of brain tumor in MRI for treatment planning. Proceedings of the 16th Annual International Conference of the IEEE Engineering in Medicine and Biology Society. (Cat. No.94CH3474-4). IEEE. Part vol.1, 1994, pp.555-6 vol.1. New York, NY, USA.

[10] Adiga PSU, Chaudhuri BB. Automatic prostate cancer grading system based on 3D histo-pathological images. Proceedings of IAPR Workshop on Machine Vision Applications. Univ. Tokyo. 1998, pp.250-3. Tokyo, Japan.

[11] W.E.L. Grimson, T. Lozano-Perez, W.M. Wells III, G.J. Ettinger, S.J. White, and R. Kikinis, "An Automatic Registration Method for Frameless Stereotaxy, Image Guided Surgery, and Enhanced Reality Visualization" In Transactions on Medical Imaging, 1996.